ORIGINAL ARTICLE

Cell Research (2007) 17: 363-373

www.nature.com/cr

PGC-1α induces apoptosis in human epithelial ovarian cancer cells through a PPARγ-dependent pathway

Yan Zhang[1,*], Yi Ba[2,*], Chang Liu[1], Guoxun Sun[1], Li Ding[1], Songyuan Gao[2], Jihui Hao[2], Zhentao Yu[2], Junfeng Zhang[1], Ke Zen[1], Zhongsheng Tong[2], Yang Xiang[1], Chen-Yu Zhang[1]

[1]State Key Laboratory of Pharmaceutical Biotechnology, School of Life Sciences, Nanjing University, Nanjing 210093, China; [2]Tianjin Medical University Cancer Institute and Hospital, Tianjin 300060, China

Peroxisome proliferator-activated receptor gamma (PPARγ) coactivator-1 alpha (PGC-1α) coactivates multiple transcription factors and regulates several metabolic processes. The current study investigated the role of PGC-1α in the induction of apoptosis in human epithelial ovarian cancer cells. The PGC-1α mRNA level between human ovaries and human ovarian epithelial tumors was examined by quantitative RT-PCR. Less PGC-1α expression was found in the surface epithelium of malignant tumors compared with normal ovaries. Overexpression of PGC-1α in human epithelial ovarian cancer cell line Ho-8910 induced cell apoptosis through the coordinated regulation of Bcl-2 and Bax expression. Microarray analyses confirmed that PGC-1α dramatically affected the apoptosis-related genes in Ho-8910 cells. Mitochondrial functional assay showed that the induction of apoptosis was through the terminal stage by the release of cytochrome *c*. Furthermore, PGC-1α-induced apoptosis was partially, but not completely, blocked by PPARγ antagonist (GW9662), and suppression of PPARγ expression by siRNA also inhibited PGC-1α-induced apoptosis in Ho-8910 cells. These data suggested that PGC-1α exerted its effect through a PPARγ-dependent pathway. Our findings indicated that PGC-1α was involved in the apoptotic signal transduction pathways and downregulation of PGC-1α may be a key point in promoting epithelial ovarian cancer growth and progression.

Keywords: PGC-1α, human epithelial ovarian cancer, apoptosis, microarray, PPARγ

Cell Research (2007) **17**:363-373. doi: 10.1038/cr.2007.11; published online 20 March 2007

Introduction

Epithelial ovarian cancer, the most common form of ovarian malignancy, is usually diagnosed at a late stage and this results in a poor prognosis [1]. The lack of preventive strategies, early diagnostic tools and effective therapies to treat the recurrent epithelial ovarian tumors prompts an urgent need to a better understanding of its pathogenesis at the molecular level [2, 3].

PGC-1α is a multiple-function transcription coactivator that regulates the activity of multiple nuclear receptors and transcription factors involved in the mitochondrial biogenesis [4, 5]. PGC-1α is widely expressed in brown fat, skeletal muscle, liver, heart, kidney and brain [6, 7]. It plays important roles in the regulation of adaptive thermogenesis in brown fat and muscle [8], muscle fiber-type switching in muscle [9], gluconeogenesis in liver [10] and insulin secretion in islets [11]. More recently, it has been found that the expression level of PGC-1α decreased in certain cancer tissues such as breast [12, 13] and colon cancers [14], suggesting that PGC-1α may be involved in the pathogenesis of cancer. In addition, the decrease of PGC-1α is always linked to the variation of peroxisome proliferator-activated receptor gamma (PPARγ) expression level [12-14]. PPARγ, a member of the nuclear receptor superfamily, forms a complex with coactivator PGCs to

*These two authors contributed equally to this work
Correspondence: Chen-yu Zhang[1], Yang Xiang[2], Zhongsheng Tong[3]
[1]Tel/Fax: +86-25-83686234; [2]Tel/Fax: +86-25-83685616
[1]E-mail: cyzhang@nju.edu.cn; [2]E-mail: xiangy@nju.edu.cn; [3]E-mail: tonghang@medmail.com.cn
Received 20 November 2006; revised 22 January 2007; accecpted 4 February 2007; published online 20 March 2007

regulate gene expression [8, 15, 16]. PPARγ has a tumorigenic role in many kinds of cancers such as colon cancer [17, 18] and mammary gland cancer [19], and activation of PPARγ signaling exacerbates the development of these tumors. On the other hand, PPARγ ligands have antiproliferative activity and induce apoptosis in many cancers [20-22]. Given that activation of PPARγ by its ligands can induce apoptosis in cancer and that PGC-1α also powerfully coactivates PPARγ, we speculate that there may be a potential relationship between PGC-1α and PPARγ in cancer development. A recent study has shown that the expression of PPARγ is indeed enhanced in epithelial ovarian carcinoma [23]; however, the role of PGC-1α in the pathogenesis of epithelial ovarian carcinoma remains to be addressed.

In the present study, we showed that PGC-1α expression in the surface epithelium of epithelial ovarian tumors was downregulated compared with normal ovaries. Overexpressing PGC-1α in human ovarian epithelial carcinoma cell line Ho-8910 significantly and specifically induced cell apoptosis through decreasing Bcl-2/Bax expression ratio and through the release of cytochrome *c*; PGC-1α exerted its effect by a PPARγ-dependent pathway. Our results reveal a new role of PGC-1α in the pathogenesis and treatment of epithelial ovarian cancer.

Materials and Methods

Human ovarian specimens

Tissue samples from 10 patients (age 46-71 years; mean age 58.2 years) with malignant epithelial ovarian tumors (four stages II and six stages III) were from the first Affiliated Hospital of Nanjing Medical University and Tissue Banking Facility of Tianjin Medical University Cancer Institute & Hospital and National Foundation for Cancer Research. All tissue samples were from patients of ovarian serous cystadenocarcinoma, which is the major type of epithelial tumors. The tumors were histopathologically diagnosed and classified assessed according to the International Federation of Gynecology and Obstetrics [24] criteria by two gynecology pathologists (WRW and DAB). Seven cases with normal ovaries from hysterectomy specimens resected for non-ovarian diseases were added and normal human ovarian surface epithelium (OSE) (age 36-55 years; mean age 45.6 years) was derived from the surface scrapings of these normal ovaries. All cases were selected based on availability of tissue and were not stratified for known preoperative or pathological prognostic factors. Following surgery, tissues were snap-frozen in liquid nitrogen and stored at –80 °C for subsequent RNA extraction.

Cell line and culture conditions

Human epithelial ovarian carcinoma cell Ho-8910 [25-27] was obtained from the Institute of Biochemistry and Cell Biology, Chinese Academy of Sciences. They were cultured in RPMI 1640 medium supplemented with 10% fetal calf serum (GBICO BRL, Rockville, MD, USA) at 37 °C in a humidified atmosphere containing 5% CO_2. Cells in the logarithmic growth phase were used for experiments.

Adenovirus infection

Recombinant adenoviruses expressing PGC-1α GFP fusion protein and GFP alone were provided by Dr Dan Kelly (Washington University, USA). Purified virus stocks were prepared through CsCl step gradient centrifugation as described previously [28]. Cells were grown to confluence, induced to differentiate for 48 h and then infected with adenovirus at a multiplicities of infection (moi) of 50. The infection efficiency was determined by GFP. Cells were harvested for isolation of total RNA or protein 48 h after infection.

Semiquantitative RT-PCR and quantitative PCR

Total RNA was isolated from Ho-8910 cells with 48 h Ad-GFP or Ad-PGC-1α infection by an RNeasy mi kit (Qiagen, Hilden, Germany). One microgram of RNA was reverse-transcribed into cDNA using oligo $(dT)_{18}$ primers and AMV reverse transcriptase (Gibco invitrogen, Carlsbad, CA, USA). PCR products of PGC-1α and house-keeping gene glyceraldehydes-3-phosphate dehydrogenase (GAPDH) were amplified with specific primers (Table 1) using the following parameters: 94 °C for 30 s, 56 °C (PGC-1α) and 59 °C (GAPDH) for 30 s and 72 °C for 30 s, with a final extension step at 72 °C for 7 min. PCR products were electrophoresed through 1.0% agarose gel, stained with ethidium bromide and visualized under ultraviolet illumination. Band intensity was calculated densitometri-cally using Quantity One-4.4.1 imaging software (Bio-Rad Laboratories). Levels of mRNA were expressed as the ratio of band intensity for PGC-1α relative to that for GAPDH.

Quantitative PCR was performed with the ABI Prism 7000 sequence detection system (Applied Biosystem, Foster City, CA) using Tagman probes (Shanghai Shinegene Molecular Biotechnology Co., Ltd), and threshold cycle numbers were obtained using ABI Prism 7000 SDS software version 1.0. The primers and probes sequences used in this study are in Table 1. Conditions for amplification were one cycle of 95 °C for 5 min followed by 40 cycles of 95 °C for 30 s, 60 °C for 1 min and final one cycle of 72 °C for 2 min.

Hoechest 33258 staining

Ho-8910 cells were infected with Ad-GFP and Ad-PGC-1α for 48 h, then cells were collected, washed with phosphate-buffered saline (PBS) and fixed by methanol-acetic acid (3:1, v/v) at 25 ºC for 10 min. Following centrifugation, the samples were washed with PBS three times, stained with Hoechest 33258 staining solution (Beyotime Biotechnology) in the dark for 5 min and then seeded separately onto cover slides. Once the treated samples had been dried in the dark at 25 ºC, stained nuclei were observed under microscope (Nikon E800).

FACS analysis

Adenovirus-infected Ho-8910 cells were subjected to single parameter analysis for apoptosis and DNA fragmentation. In brief, cells were washed with PBS and suspended in 100% ethanol at 4 °C overnight. Fixed cells were then centrifuged at 1000 r.p.m. and treated with hypotonic fluorochrome solution, containing 0.1% sodium citrate, 0.1% Triton-X-100 and 50 mg/ml propidium iodide (PI) according to the procedure of Nicoletti *et al.* [29]. Treated nuclei were stained 30 min at 4 °C, while protected from light and washed with PBS three times. The PI fluorescence of individual nuclei was measured by a FACSort flow cytometer (Becton-Dickinson, San Jose, CA,USA). Stained cells traversed the 488 nm argon laser at an event rate of approximately 400 nuclei/s and it was maintained for all samples analyzed. A 585/42 nm

Table 1 PCR primers used in this study

mRNA	Primer
Homo PGC-1α mRNA (465 bp, RT-PCR)	Sense primer: 5′-TCCCGATCACCATATTCC-3′ Anti-sense primer: 5′-TTCAAGAGCAGCAAAAGC-3′
Homo GAPDH mRNA (383 bp, RT-PCR)	Sense primer: 5′-ATCCCATCACCATCTTCCAG-3′ Anti-sense primer: 5′-CCATCACGCCACAGTTTCC-3′
Homo PGC-1α mRNA (quantitative RT-PCR)	Sense primer: 5′-GTCACCACCCAAATCCTTAT-3′ Anti-sense primer: 5′- ATCTACTGCCTGGAGACCTT-3′ Probe: 5′FAM + ATATGGTGATCGGGAACACGACC + TAMRA3′
Homo PPARγ mRNA (quantitative RT-PCR)	Sense primer: 5′-GGCTTCATGACAAGGGAGTTTC-3′ Anti-sense primer: 5′-AACTCAAACTTGGGCTCCATAAAG-3′ Probe:5′FAM + AAAGAGCCTGCGAAAGCCTTTTGGTG+TAMRA3′
Homo Bax mRNA (quantitative RT-PCR)	Sense primer: 5′-CATGTTTTCTGACGGCAACTTC-3′ Anti-sense primer: 5′-AGGGCCTTGAGCACCAGTTT-3′ Probe: 5′FAM + CCGGGTTGTCGCCCTTTTCTACTTTG + TAMRA3′
Homo Bcl-2 mRNA (quantitative RT-PCR)	Sense primer: 5′-GGTGGTGGAGGAGCTCTTCA-3′ Anti-sense primer: 5′-TGACGCTCTCCACACACATGA-3′ Probe: 5′ FAM + AGGATTGTGGCCTTCTTTGAGTT + TAMRA3′
Homo GAPDH mRNA (quantitative RT-PCR)	Sense primer: 5′-CCACTCCTCCACCTTTGAC-3′ Anti-sense primer: 5′-ACCCTGTTGCTGTAGCCA-3′ Probe: 5′FAM + TTGCCCTCAACGACCACTTTGTC + TAMRA3′

band pass filter was used to collect the red fluorescence from PI-stained nuclei and the data recorded in the linear scale. A minimum of 10 000 events were collected for each analysis. The percentage of apoptotic nuclei (sub-diploid DNA peak in the DNA fluorescence histogram) was calculated with Cell Quest software (Becton-Dickinson, San Jose, CA, USA).

Electron microscopy

Adenovirus-infected Ho-8910 cells were detached from the plates with a cell lifter and centrifuged at 1 000 r.p.m. for 5 min. The cell pellet was first fixed with 2.5% glutaraldehyde in 0.1 M PBS (pH 7.4) for 2 h at 4 °C and then post-fixed in 1% osmium tetroxide, 0.1 M phosphate buffer (pH 7.4). After dehydration in ethanol and embedded in an Epon-Araldite mixture, thin sections were obtained with a Reichert-Jung Ultracut-E ultramicrotome and stained with lead citrate. Samples were examined with a JEM-EX electron microscope (JEOL, Tokyo, Japan).

Western blot analysis

Cytosolic-specific, mitochondria-free lysates were prepared as described in Miyake *et al.* [30]. After 48 h adenovirus infection, Ho-8910 cells were collected by centrifugation at 600 × *g* for 5 min. The cell pellet was lysed on ice in 300 μl of a chilled hypotonic lysis solution (220 mM mannitol, 68 mM sucrose, 50 mM PIPES-KOH (pH 7.4), 50 mM KCl, 5 mM EDTA, 2 mM $MgCl_2$, 1 mM dith-iothreitol and a mixture of protease inhibitors consisting of 100 μM 4-(2-amoethyl)-benzenesulfonyl fluoride, 80 nM aprotinin, 5 μM bestatin, 1.5 μM E-64 protease inhibitor, 2 μM leupeptin and 1 μM pepstatin A). After 45 min incubation on ice, the cell lysates were centrifuged at 600 × *g* for 10 min. The supernatant was collected in a microcentrifuge tube and centrifuged at 14 000 r.p.m. for 30 min. Protein concentration was determined by the BCA method (Pierce, Rockford, USA). For electrophoresis, equal amounts of proteins (60 μg) were loaded onto 15% SDS-PAGE gels. After electrophoresis, protein bands were transferred to nitrocellulose membranes. The membranes were blocked with TBST containing 5% non-fat milk (blocking buffer) for 1 h and then incubated with anti-cytochrome *c* antibody (Santa Cruz Biotechnology, Santa Cruz, USA) diluted 1:1 000 in blocking buffer at 4 °C overnight. After washing three times with TBST, the membranes were incubated with HRP-conjugated goat anti-mouse IgG antibody (Santa Cruz; diluted 1:2 000) for 1 h at room temperature. The immunoblots were visualized by

an enhanced chemiluminescence detection system (NEN, Boston, USA).

Microarray assay

Total RNA of adenovirus-infected Ho-8910 cells were isolated using Trizol reagent (Invitrogen) and analyzed by a human genome 70-mer oligonucleotide microarray from CapitalBio Corporation (Beijing, China). Briefly, a Human Genome Oligo Set Version 2.0 consisting of 5′-amo-modified 70-mer probes and representing 21 329 well-characterized *Homo sapiens* genes was purchased from Qiagen and printed on amo-silaned glass slides. A space- and intensity-dependent normalization based on a LOWESS program [31] was employed. Three independent experiments were performed, and for each test and control sample, two hybridizations were performed by using a reversal fluorescent strategy. Only genes whose alteration tendency kept consistency in both microarray assays were selected as differentially expressed genes.

siRNA interference

Three siRNA sequences targeting different sites of human PPARγ cDNA were designed and synthesized by Genesil (Wuhan, PR China). Control sequence that could not target PPARγ cDNA was also included as a negative control. siRNA was transfected into Ho-8910 cells using LipofectAmine reagent (Gibco-Invitrogen) according to the manufacturer's manual. At 48 h after medium replace-ment, cells were harvested for total RNA isolation, and PPARγ expression level was analyzed by quantitative PCR. The primer sequences used in the experiments are detailed in Table 1. The sequence with the best interfering effect (named S1) was selected. siRNA sequences were as follows: S1, AAGATGACAGACCTCAGGCAG; S2, AAACCCTT-TACCACGGTTGAT; S3, AACTTCGG-AATCAGCTCTGTG; N (the negative control sequence), ACTACCGTTGTTATAGGTG.

Statistical analysis

All experiments were performed in triplicate and the results are expressed as means ± S.E.M. Statistical analyses were performed using SPSS/Windows version 12.5S statistical package (SPSS, Chicago, IL, USA). Statistical significance was accepted at the level of $p < 0.05$.

Results

Expression of PGC-1α is downregulated in epithelial ovarian cancer

To investigate PGC-1α expression in normal human ovaries and human ovarian epithelial tumors, quantitative RT-PCR was used to assess the levels of PGC-1α mRNA in normal ovaries (n = 7) and tumor tissues (n = 10), and the results were normalized against the GAPDH mRNA. Results showed that the PGC-1α mRNA level in surface epithelium decreased to 41 ± 8% in ovarian tumors as compared with normal tissues (Figure 1).

Overexpression of PGC-1α in Ho-8910 cells induces cell apoptosis

As shown in Figure 2A, moi of 50 for both Ad-GFP and Ad-PGC-1α resulted in 80-90% infection efficiency. RT-PCR analysis showed that PGC-1α expression was upregulated by 3.5-fold in Ad-PGC-1α-infected Ho-8910 cells as compared with the control group (Figure 2B).

To investigate the effect of elevated PGC-1α on ovarian tumor cells, morphological changes were observed under phase contrast and light microscopes. At 48 h after infection, Ad-GFP-infected and control cells maintained normal morphology. In contrast, Ad-PGC-1α-infected Ho-8910 cells exhibited cell shrinkage, condensed chromatin, loss of cell-to-cell contact and had in part detached from the plate. Many of these characteristics were suggestive of apoptosis. We thus further characterized the phenomena by Hoechest staining assay, and our results showed that apoptotic bodies containing nuclear fragments were only found in Ad-PGC-1α-infected cells (73%) as compared with control and mock vector infected cells (Ad-GFP group) (Figure 3A).

To further confirm the effect of PGC-1α on apoptosis, cell slides were analyzed by electron microscopy. Results as shown in Figure 3B demonstrated that typical chromatin condensation and disappearance of nuclear ultrastructure occurred when a high level of PGC-1α was expressed in Ho-8910 cells. No such phenomenon was observed in cells infected with the control vector.

We subsequently used fluorescence-activated cell sorting (FACS) to investigate how PGC-1α affected cell apoptosis at various time points after its forced expression. In this study, as the expression of PGC-1α increased, majority of the cells entered apoptosis. From 0 to 24 h post-infection, the sub-diploid nuclei indicative of apoptosis appeared

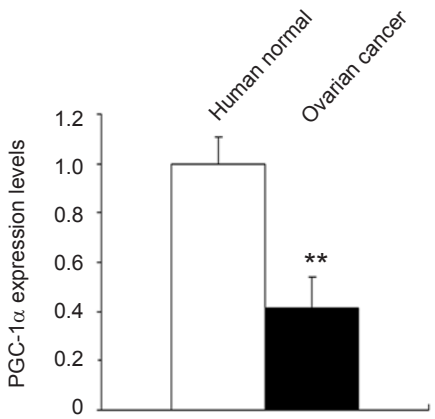

Figure 1 PGC-1α mRNA levels in normal human ovaries and ovarian tumors. PGC-1α expression levels in the OSE were determined by quantitative RT-PCR and quantified as the ratio of PGC-1α/GAPDH. Data of normal ovaries (n = 7) and ovarian tumors (n = 10) were expressed as means ± S.E.M. PGC-1α expression levels were quantified as the ratio to GAPDH and the values of PGC-1α/GAPDH were normalized to that of control. $^{**}p < 0.01$ compared with control.

(32.7%) in Ad-PGC-1α-infected cells, and at 48 h the sub-diploid nuclei were further increased to 58.9%. In contrast, Ad-GFP-infected cells were not significantly influenced and showed a similar profile as control cells. Taken together, our results clearly showed a distinct apoptosis induced by PGC-1α in Ho-8910 cells compared with the control group. Thus, overexpression of PGC-1α suppressed cancer cell growth and induced massive cell death by apoptosis.

Differential gene expression induced by overexpressed PGC-1α in Ho-8910 cells

To further investigate genes that contribute to PGC-1α-induced apoptosis in Ho-8910 cells, we performed a global gene expression analysis by the standard microarray technology. A total of 1 998 genes were altered in Ho-8910 cells overexpressing PGC-1α. Among those altered genes, 1 057 genes were downregulated and 941 genes were upregulated. Many apoptosis-inducing genes were found in the upregulated group while apoptosis-restraining genes were in the downregulated group. For instance, the expression level of Bcl-2 was suppressed while Bax was increased (Figure 4A). Other pro-apoptotic genes of the Bcl-2 family including Bak1, Hrk, Bcl-2l11, Bcl-2l1, Bcl-2l13 were also upregulated (Figure 4A). The expression level of caspase family such as the apoptotic effector caspase 3 also changed (Figure 4B). Genes involved in DNA fragmentation were significantly upregulated. For example, the levels of CIDE3, CIDEA and DFFA were increased 8-, 4- and 2-, respectively (Figure 4C). In contrast, several IAP (inhibitor of apoptosis protein) family genes such as BIRC3, BIRC5 and BIRC1 were all downregulated (Figure 4D). Other genes involved in the apoptosis pathway showed altered expressions, too (Figure 4E). Our array data suggested that increased expression of PGC-1α in Ho-8910 cells affected many genes involved in apoptosis.

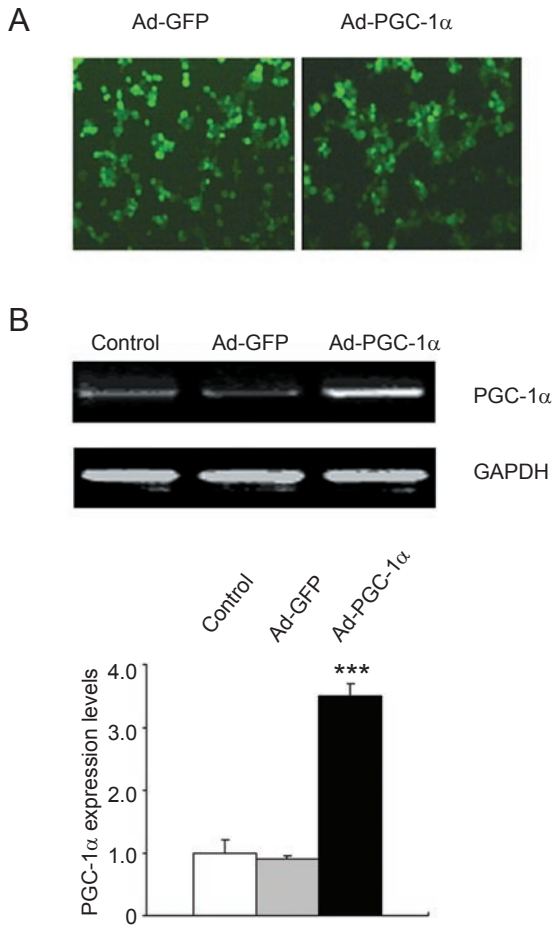

Figure 2 The expression levels of PGC-1α in recombinant adenovirus-infected Ho-8910 cells. Ho-8910 cells were infected with Ad-GFP and Ad-PGC-1α at a moi of 50 for 48 h. **(A)** Fluorescent photos of Ho-8910 cells after infection. **(B)** Representative RT-PCR analysis for PGC-1α in Ho-8910 cells. Lane 1, normal Ho-8910 cells, Lane 2, Ho-8910-infected Ad-GFP, Lane 3, Ho-8910 infected by Ad-PGC-1α. **(C)** PGC-1α expression levels were quantified as the ratio to GAPDH and the values of PGC-1α/GAPDH were normalized to that of control. ***$p < 0.001$ compared with control.

PGC-1α overexpression in Ho-8910 cells alters Bcl-2 and Bax expression and increases cytochrome c release

To validate the microarray results, the expression ratio of the anti-apoptotic gene Bcl-2 versus pro-apoptotic gene Bax was analyzed by quantitative RT-PCR. As shown in Figure 5A, Bcl-2 expression in Ad-PGC-1α infected Ho-8910 cells was significantly decreased (by ~69%) compared with the control group, whereas Bax expression was increased by 1.5-fold after Ad-PGC-1α infection. In contrast, no changes of Bcl-2 and Bax expression were observed in the Ad-GFP group. We also examined the cytochrome *c* protein level in the cytoplasm. Overexpression of PGC-1α caused significant increase of cytochrome *c* level in Ho-8910 cells compared with the Ad-GFP group (Figure 5B). The significant decrease of Bcl-2/Bax ratio and the increase of cytochrome *c* level in the cytoplasm are consistent with the induction of apoptosis in Ad-PGC-1α-infected Ho-8910 cells.

PPARγ antagonist suppresses PGC-1α-induced apoptosis in Ho-8910 cells

Since PPARγ ligands induce apoptosis in many cancers [17-19] and PGC-1α powerfully coactivates PPARγ [8], we asked whether PGC-1α-induced apoptosis in Ho-8910 cells is mediated by a PPARγ-dependent pathway.

Ho-8910 cells infected with the GFP or PGC-1α adenovirus were immediately treated with 10 μM GW9662, an irreversible PPARγ antagonist, for 48 h followed by Hoechest staining. As shown in Figure 6, the number of apoptotic

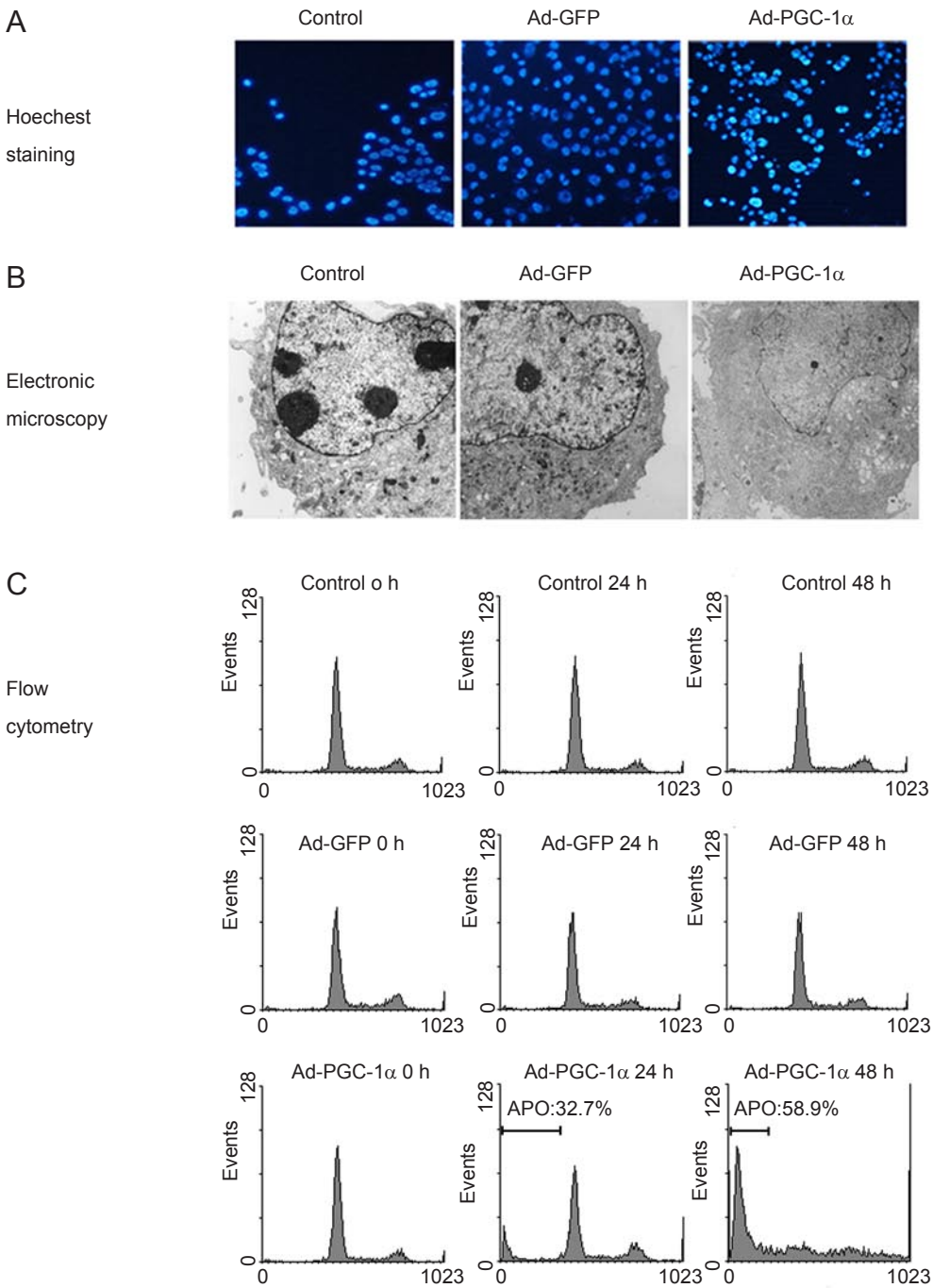

Figure 3 Detection of PGC-1α-induced apoptosis in Ho-8910 cells. **(A)** Hoechest 33258 staining of Ho-8910 cells. From Left to Right: Control, Ad-GFP, Ad-GFP-PGC-1α (fluorescence microscope, 400×). **(B)** Transmission electron microscopy of cells infected by Ad-PGC-1α. From Left to Right: Control, Ad-GFP, Ad-PGC-1α (original magnification, 3000×). **(C)** Representative flow cytometry profiles of either uninfected or infected Ho-8910 cells. From Top to Bottom: Control (0, 24 and 48 h), Ad-GFP (0, 24 and 48 h), Ad-GFP-PGC-1α (0, 24 and 48 h).

cells decreased by about 50-60% in Ad-PGC-1α-infected Ho-8910 cells after 10 μM GW9662 treatment compared with untreated cells, suggesting that PPARγ antagonist GW9662 partially, but not completely, blocked PGC-1α-induced Ho-8910 cell apoptosis. This result suggests that PGC-1α exerted its effect through PPARγ-dependent and

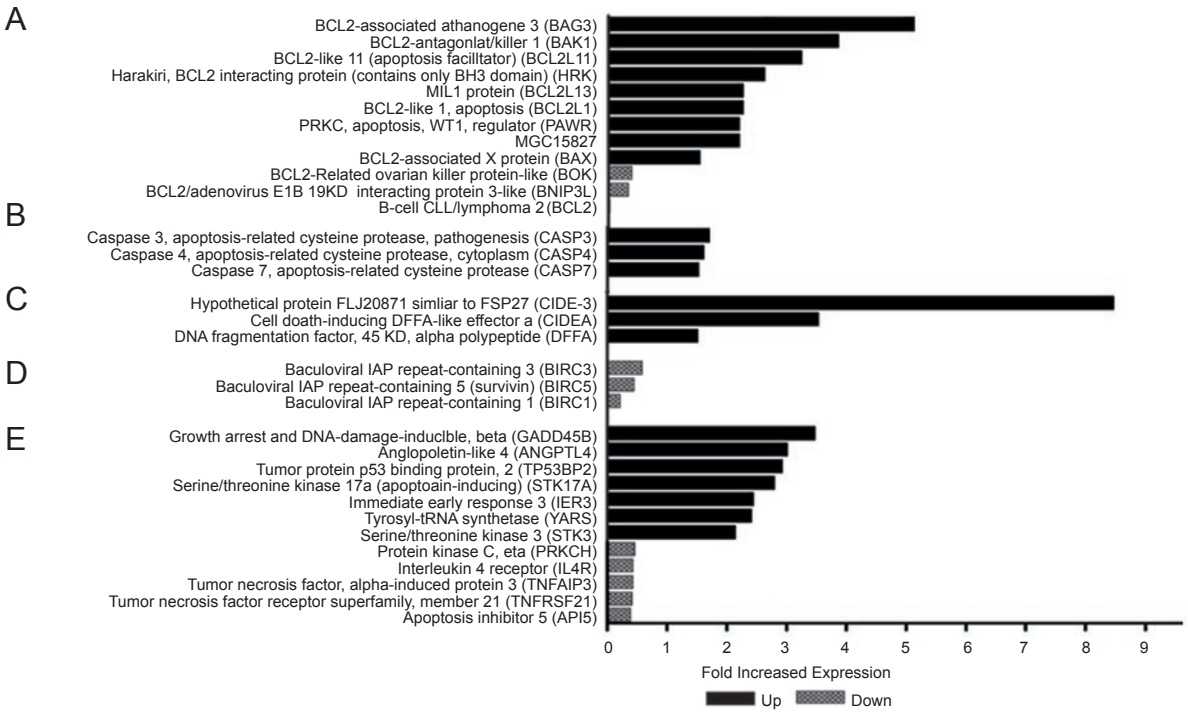

Figure 4 Differential expression of apoptosis-related genes in PGC-1α-overexpressed Ho-8910 cells. **(A)** Bcl-2 family members. **(B)** Caspase family members. **(C)** DNA fragmentation gene. **(D)** IAP (inhibitor of apoptosis protein) family genes. **(E)** Others. Black bars are the genes upregulated with the ratio =1.5, while gray bars are the genes downregulated with the ratio =0.6. Three independent experiments were performed, and for each test and control sample, two hybridizations were performed by using a reversal fluorescent strategy.

-independent pathways.

Suppression of PPARγ inhibits the PGC-1α-induced apoptosis in Ho-8910 cells

To further test our hypothesis that PGC-1α-induced apoptosis occurs through PPARγ-dependent pathway, we knocked down PPARγ expression in Ho-8910 cells by using siRNA interference. As shown in Figure 7, siRNA S1 inhibited PPARγ expression by 35-40% in Ho-8910 cells as compared to negative control (siRNA N). The decrease of PPARγ expression also inhibited PGC-1α-induced apoptosis in Ho-8910 cells, and the number of apoptotic cells decreased by about 70-80% compared with groups that did not receive siRNA S1 (Figure 8). This result supported our interpretation that PGC-1α-induced apoptosis in Ho-8910 cells occurs through a PPARγ-dependent pathway.

Discussion

The OSE is thought to be the origin of most ovarian cancers in human. Greater than 90% of ovarian cancer arises from the transformation of OSE [32]. Therefore, study of the pathogenesis of epithelial ovarian cancer is very important in ovarian cancer therapy. Recent report shows that the expression of PPARγ is significantly enhanced in the late-stage epithelial ovarian carcinoma, indicating that PPARγ contributes significantly to the onset and progression of ovarian cancer [33]. Because the levels of PPARγ and the PPARγ coactivator, PGC-1α, are always linked to clinical outcome in patients with a variety of human cancers [12-14], it is reasonable to suspect that PGC-1α may also play a pivotal role in the pathogenic development of epithelial ovarian cancer. However, no correlation has been established for the possible involvement of PGC-1α in ovarian cancer. In this study, we first demonstrated that PGC-1α mRNA level was significantly decreased in late-stage human epithelial ovarian cancer compared with normal ovarian tissues. This finding is also consistent with others reports and our own studies showing that PGC-1α is downregulated in breast cancer [12, 13], colon cancer [14], liver cancer and hypothyroid cancer (data not shown). Therefore, a better understanding of PGC-1α's effect on epithelial ovarian cancer may have important implications for the treatment of this disease in clinics.

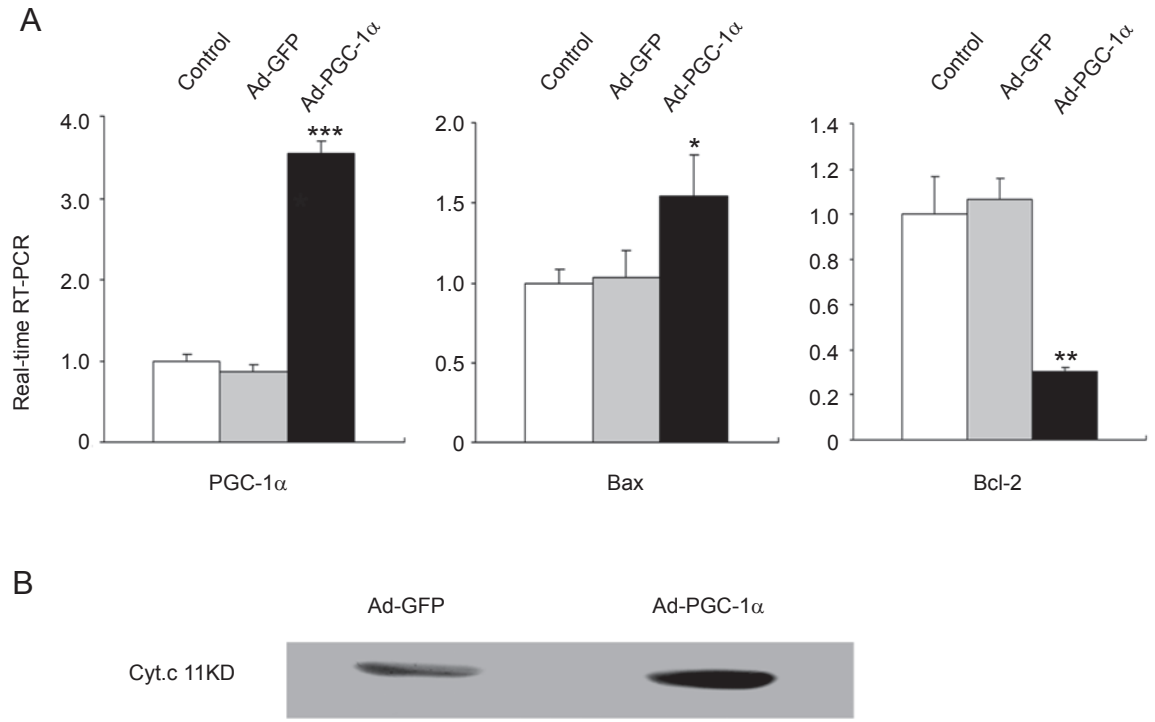

Figure 5 (A) Bcl-2 and Bax expression in Ad-PGC-1α-infected Ho-8910 cells. Total RNA was extracted from Ho-8910 cells either uninfected or infected for 48 h and subjected to quantitative RT-PCR. From Left to Right: PGC-1α, Bax, Bcl-2. Data (n = 9) are expressed as means ± S.E.M. Gene expression levels were quantified as the ratio to GAPDH and the ratio values were normalized to that of control.*$p < 0.05$, **$p < 0.01$, ***$p < 0.001$ compared with controls. **(B)** Effect of PGC-1α on cytochrome *c* release in Ho-8910 cells. Ho-8910 cells were treated with GFP or PGC-1α adenovirus vehicle for 48 h. Cytosol-specific, mitochondria-free lysates were prepared. An equivalent amount of protein (60 μg) from individual lysates were electrophoresed, and probed by Western blot with anti-cytochrome *c* antibody.

Our human epithelial ovarian cancer samples were collected from patients of ovarian serous cystadenocarcinomas; thus, the Ho-8910 cell line, which also originated from human ovarian serous cystadenocarcinoma [34], would be a suitable model for *in vitro* study. Since PGC-1α was downregulated in epithelial ovarian cancer, we upregulated PGC-1α expression in epithelial ovarian cancer cell line Ho-8910 by adenovirus infection to examine the potential effect. Strikingly, we found that elevated PGC-1α induced cell apoptosis. PGC-1α has been shown to stimulate mitochondrial biogenesis and respiration in muscle cells [8], to stimulate the hepatic gluconeogenesis in liver [10] or to regulate insulin secretion in islets [11]. There has been no previous reports showing that PGC-1α can induce apoptosis in cancer. The current findings uncovered a new function of PGC-1α in tumorigenesis, especially in ovarian cancer. The fact that PGC-1α expression decreases in ovarian cancer *in vivo* and the increase of PGC-1α expression promotes apoptosis of ovarian cancer cell *in vitro* suggests that PGC-1α might be closely involved in the pathogenesis of the epithelial ovarian cancer.

To address the mechanisms involved in PGC-1α-induced apoptosis in Ho-8910 cells, the mRNA levels of Bax and Bcl-2 were analyzed by quantitative PCR. Pro-apoptotic gene Bax and anti-apoptotic gene Bcl-2 are known as Bcl-2 family members, which are the central regulator of apoptosis [35], and the opposing functions of anti- and pro-apoptotic members arbitrate the life-or-death decision [36]. The ratio of Bcl-2 to Bax is important in determining susceptibility to apoptosis and is usually regarded as a criterion in programmed cell death [37]. Our results revealed that Bcl-2 was markedly downregulated while Bax was concurrently upregulated in PGC-1α-overexpressed Ho-8910 cells, suggesting that PGC-1α-induced apoptosis is mediated by a decreasing ratio of Bcl-2/Bax. The change of Bcl-2/Bax can destabilize mitochondria, leading to the release of several mitochondrial intermembrane space proteins such as cytochrome *c* into the cytosol where they

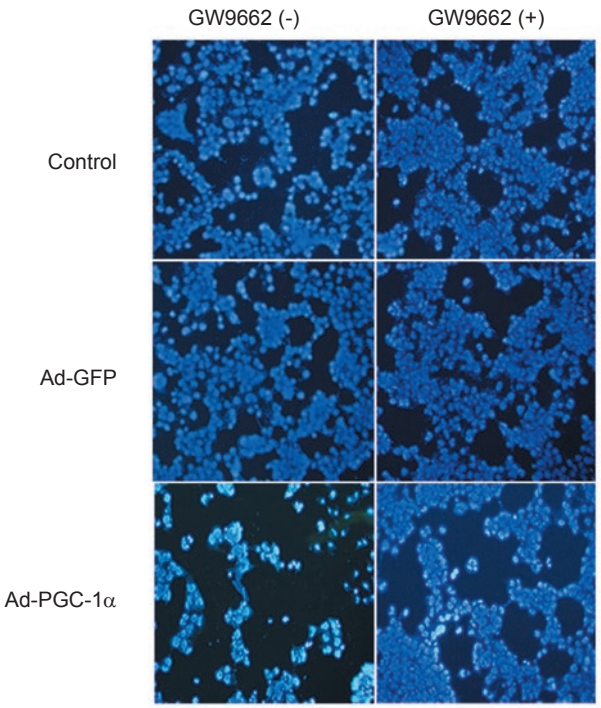

Figure 6 Effect of PPARγ antagonist on PGC-1α-induced apoptosis in Ho-8910 cells. Ho-8910 cells were infected with the GFP or PGC-1α adenovirus vehicles in either the absence (-) or presence (+) of 10 μM GW9662. After 48 h, apoptosis was assayed by Hoechest 33258 staining. From Top to Bottom: Control, Ad-GFP, Ad-PGC-1α. (fluorescence microscope, 100×).

actively trigger the process of programmed cell death [38, 39]. Indeed, we found that exogenous PGC-1α can induce cytochrome *c* release from mitochondria into the cytosol in Ho-8910 cells.

In addition, our microarray analysis also indicated that the expressions of many apoptosis-related genes were markedly changed in PGC-1α-infected Ho-8910 cells, particularly the Bcl-2 family genes such as Bak, Hrk, Bcl2l1, Bcl2l11 and Bcl2l13. It was most likely that PGC-1α-induced apoptosis was mediated by the Bcl-2 family in Ho-8910 cells. The change of pro-apoptotic/anti-apoptotic member ratio then triggered the cytochrome *c* release from mitochondria to the cytosol, leading to downstream apoptosis. The mechanism by which this set of apoptosis-related genes was coordinately regulated by PGC-1α may be related with PPARγ, because PGC-1α powerfully coactivates PPARγ and the activation of PPARγ can also induce apoptosis through Bcl-2 family members in cancers [40-43]. To investigate whether PGC-1α-induced apoptosis is mediated through PPARγ, we utilized the PPARγ antigonist GW9662 to block the action of PPARγ. Results showed that GW9662 can partially inhibit PGC-1α-induced apoptosis in Ho-8910 cells, suggesting that PGC-1α may facilitate apoptosis through a PPARγ-dependent pathway. Since this antagonist has some off-target activity, we sup-

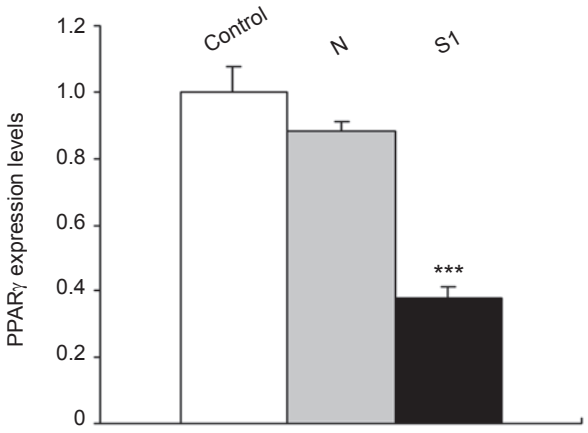

Figure 7 The expression level of PPARγ in siRNA-infected Ho-8910 cells. Ho-8910 cells were transfected with siRNA S1 or the negative control (siRNA N). The interference effect was analyzed by quantitative PCR. Data were shown as the ratio of PPARγ/GAPDH. Individual data points in this figure represent the means ± S.E.M. of 18 determinants from three independently prepared samples each with six measurements. ***$p < 0.001$ compared with the control or N group.

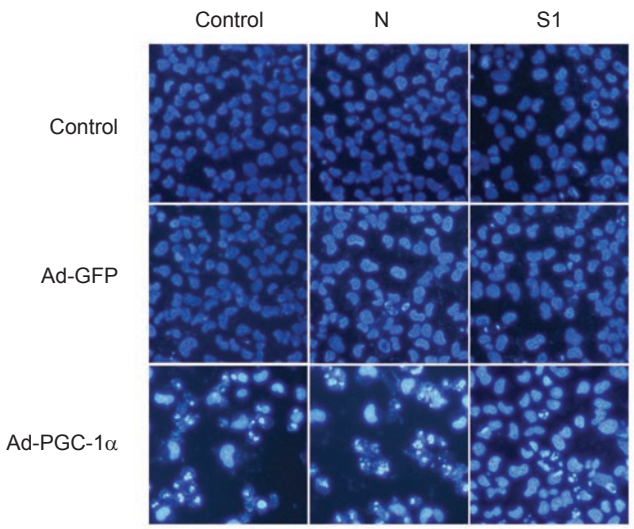

Figure 8 Effect of suppressed PPARγ expression on PGC-1α-induced apoptosis in Ho-8910 cells. Ho-8910 cells were infected with the GFP or PGC-1α adenovirus vehicles 48 h after the treatment with siRNA S1 or the negative control (siRNA N). Apoptosis was assayed by Hoechest 33258 staining. From Top to Bottom: Control, Ad-GFP, Ad-PGC-1α; From Left to Right: Control, N, S1 (fluorescence microscope, 400×).

pressed PPARγ expression by siRNA, and found that this also inhibited PGC-1α-induced apoptosis in Ho-8910 cells, supporting our interpretation that PGC-1α exerted its effect through a PPARγ-dependent pathway. Although PPARγ is upregulated in epithelial ovarian carcinoma [23], the downregulation of PGC-1α in epithelial ovarian cancer may restrain the activation of PPARγ-dependent apoptotic pathway, which could indirectly contribute to the development of ovarian tumor. However, the detailed molecular mechanisms need further study. In addition, due to difficulties to obtain normal human ovarian tissues or cells, the specificity of cytotoxic effects of PGC-1α on ovarian cancers remains to be addressed.

In summary, our current study provides the first evidence that the expression of PGC-1α is downregulated in human epithelial ovarian cancer and that the overexpre-ssion of PGC-1α can induce apoptosis in human ovarian epithelial cancer cell line Ho-8910. The cytotoxic effect of PGC-1α on ovarian cancer cells may be useful for cancer therapy.

Acknowledgments

We thank Rongxi Sun from The first Affiliated Hospital of Nanjing Medical University for kindly providing the human ovarian specimens. This work was supported by grants from the National Natural Science Foundation of China (No. 30225037, 30400538, 30471991, 30570731), the 973 Program of China (No. 2006CB503909, 2004CB518603), the "111" Project, and the Natural Science Foundation of Jiangsu Province (No. BK2004082, BK2006714).

References

1 Jemal A, Thomas A, Murray T, Thun M. Cancer statistics. CA Cancer J Clin 2002; **52**:23-47.
2 Wooster R, Weber BL. Breast and ovarian cancer. N Engl J Med 2003; **348**:2339-2347.
3 Zhang L, Conejo-Garcia JR, Katsaros D, *et al*. Intratumoral T cells, recurrence, and survival in epithelial ovarian cancer. N Engl J Med 2003; **348**:203-213.
4 Puigserver P, Spiegelman BM. Peroxisome proliferator-activated receptor-coactivator 1α (PGC-1α): transcriptional coactivator and metabolic regulator. Endocr Rev 2003; **24:**78-90.
5 Wu Z, Puigserver P, Andersson U, *et al*. Mechanisms controlling mitochondrial biogenesis and respiration through the thermogenic coactivator PGC-1. Cell 1999; **98**:115-124.
6 Larrouy D, Vidal H, Andreelli F, Laville M, Langin D. Cloning and mRNA tissue distribution of human PPARgamma coactivator-1. Int J Obes Relat Metab Disord 1999; **23**:1327-1332.
7 Esterbauer H, Oberkofler H, Krempler F, Patsch W. Human peroxisome proliferator activated receptor gamma coactivator 1 (PPARGC1) gene: cDNA sequence, genomic organization, chromosomal localization, and tissue expression. Genomics 1999; **62**:98-102.
8 Puigserver P, Wu Z, Park CW, Graves R, Wright W, Spiegelman BM. A cold-inducible coactivator of nuclear receptors linked to adaptive thermogenesis. Cell 1998; **92**:829-839.
9 Lin J, Wu H, Tarr PT, *et al*. Transcriptional co-activator PGC-1α drives the formation of slow-twitch muscle fibres. Nature 2002; **418**:797-801.
10 Yoon JC, Puigserver P, Chen G, *et al*. Control of hepatic gluconeogenesis through the transcriptional coactivator PGC-1. Nature 2001; **413**:131-138.
11 Yoon JC, Xu G, Deeney JT, *et al*. Suppression of β cell energy metabolism and insulin release by PGC-1α. Dev Cell 2003; **5**:73-83.
12 Jiang WG, Douglas-Jones A, Mansel RE. Expression of peroxisome-proliferator activated receptor-gamma (PPARgamma) and the PPARgamma co-activator, PGC-1, in human breast cancer correlates with clinical outcomes. Int J Cancer 2003; **106**:752-757.
13 Watkins G, Douglas-Jones A, Mansel RE, Jiang WG. The localisation and reduction of nuclear staining of PPARgamma and PGC-1 in human breast cancer. Oncol Rep 2004; **12**:483-488.
14 Feilchenfeldt J, Brundler MA, Soravia C, Totsch M, Meier CA. Peroxisome proliferator-activated receptors (PPARs) and associated transcription factors in colon cancer: reduced expression of PPARgamma-coactivator 1 (PGC-1). Cancer Lett 2004; **203**:25-33.
15 Castillo G, Brun RP, Rosenfield JK, *et al*. An adipogenic cofactor bound by the differentiation domain of PPAR gamma. EMBO J 1999; **18**:3676-3687.
16 Puigserver P, Adelmant C, Wu ZD, *et al*. Activation of PPAR gamma coactivator-1 through transcription factor docking. Science 1999; **286**:1368-1371.
17 Lefebvre AM, Chen I, Desreumaux P, *et al*. Activation of the peroxisome proliferator-activated receptor γ promotes the development of colon tumors in C57BL/6J-APCMin/+ mice. Nat Med 1998; **4**:1053-1057.
18 Saez E, Tontonoz P, Nelson MC, *et al*. Activators of the nuclear receptor PPARγ enhance colon polyp formation. Nat Med 1998;**4**:1058-1061.
19 Saez E, Rosenfeld J, Livolsi A, *et al*. PPARγ signaling exacerbates mammary gland tumor development. Genes Dev 2004;**18**:528-540.
20 Koeffler HP. Peroxisome proliferator-activated receptor gamma and cancers. Clin Cancer Res 2003; **9**:1-9.
21 Park BH, Breyer B, He TC. Peroxisome proliferator-activated receptors: roles in tumorigenesis and chemoprevention in human cancer. Curr Opin Oncol 2001; **13**:78-83.
22 Rumi MA, Ishihara S, Kazumori H, Kadowaki Y, Kinoshita Y. Can PPAR gamma ligands be used in cancer therapy? Curr Med Chem Anticancer Agents 2004; **4**:465-477.
23 Zhang GY, Ahmed N, Riley C, *et al*. Enhanced expression of peroxisome proliferator-activated receptor gamma in epithelial ovarian carcinoma. Br J Cancer 2005; **92**:113-119.
24 No authors listed. International Federation of Gynecology, and Obstetrics: changes in definitions of clinical staging for carcinoma of the cervix and ovary. Am J Obstet Gynecol 1987; **156**:263-264.
25 Mou Z, Xu SH, Zhang YY. Constitution of human ovarian cancer cell line HO8910 and its biological characteristic. Zhong Hua Fu Chan Ke Za Zhi 1994; **29**:162-164.
26 Ma W, Yu H, Wang Q, Bao J, Yan J, Jin H. In vitro biological

activities of transmembrane superantigen staphylococcal enterotoxin A fusion protein. Cancer Immunol Immunother 2004; **53**:118-124.
27 Zhang J, Wang X, Tu C, *et al*. Monofunctional platinum complexes showing potent cytotoxicity against human liver carcinoma cell line BEL-7402. J Med Chem 2003; **46**:3502-3507.
28 Miyake S, Makimura M, Kanegae Y, *et al*. Efficient generation of recombinant adenoviruses using adenovirus DNA-termal protein complex and a cosmid bearing the full-length virus genome. Proc Natl Acad Sci USA 1996; **93**:1320-1324.
29 Nicoletti I, Migliorati G, Pagliacci M, Grignani F, Riccardi C. A rapid and simple method for measuring thymocyte apoptosis by propidium iodide staining and flowcytometry. J Immunol Methods 1991; **139**:271-279.
30 Yang CC, Lin HP, Chen CS, Yang YT, Tseng PH, Rangnekar VM. Bcl-xL mediates a survival mechanism independent of the phosphoinositide 3-kinase/Akt pathway in prostate cancer cells. J Biol Chem 2003; **278**:25872-25878.
31 Yang YH, Dudoit S, Luu P, *et al*. Normalization for cDNA microarray data: a robust composite method addressing single and multiple slide systematic variation. Nucleic Acids Res 2002; **30**: e15.
32 Choi KC, Auersperg N. The ovarian surface epithelium: simple source of a complex disease. Minerva Ginecol 2003; **55**:297-314.
33 Zhang GW, Ahmed N, Riley C, *et al*. Enhanced expression of peroxisome proliferator-activated receptor gamma in epithelial ovarian carcinoma. Br J Cancer 2005; **92**:113-119.
34 Hu ZY, Deng XG. Effects of progesterone to human ovarian cancer cell line HO8910's proliferation and apoptosis. Zhong Hua Fu Chang Ke Za Zhi 2000; **35**:423-426.
35 Shen ZN, Nishida K, Doi H, *et al*. Suppression of chondrosarcoma cells by 15-deoxy-Delta 12,14-prostaglandin J2 is associated with altered expression of Bax/Bcl-xL and p21. Biochem Biophys Res Commun 2005; **328**:375-382.
36 Cory S, Adams JM. The Bcl2 family: regulators of the cellular life-or-death switch. Nat Rev Cancer 2002; **2**:647-656.
37 Korsmeyer SJ, Shutter JR, Veis DJ, Merry DE, Oltvai ZN. Bcl-2/Bax: a rheostat that regulates an anti-oxidant pathway and cell death. Semin Cancer Biol 1993; **4**:327-332.
38 Cai J, Yang J, Jones DP. Mitochondrial control of apoptosis: the role of cytochrome *c*. Biochim Biophys Acta 1998; **1366**:139-149.
39 Tsujimoto Y. Cell death regulation by the bcl-2 protein family in the mitochondria. J Cell Physiol 2003; **195**:158-167.
40 Shiau CW, Yang CC, Kulp SK, *et al*. Thiazolidenediones mediate apoptosis in prostate cancer cells in part through inhibition of Bcl-xL/Bcl-2 functions independently of PPARgamma. Cancer Res 2005; **65**:1561-1569.
41 Kang HY, Lee JY, Lee JS, Choi YM. Peroxisome proliferator-activated receptors-gamma activator, ciglitazone, inhibits human melanocyte growth through induction of apoptosis. Arch Dermatol Res 2006; **297**:472-476.
42 Li MY, Deng H, Zhao JM, Dai D, Tan XY. PPARgamma pathway activation results in apoptosis and COX-2 inhibition in HepG2 cells. World J Gastroenterol 2003; **9**:1220-1226.
43 Bogazzi F, Russo D, Locci MT, *et al*. Apoptosis is reduced in the colonic mucosa of patients with acromegaly. Clin Endocrinol (Oxf) 2005; **63**:683-688.